MEMORANDUM REPORT BRL-MR-3725

(SUPERSEDES IMR-855)

BRL

1938 – Serving the Army for Fifty Years – 1988

PRESSURE MEASUREMENTS ON THE INTERIOR SURFACE OF A 75MM TUBULAR PROJECTILE AT MACH 4

LYLE D. KAYSER
RAO J. YALAMANCHILI
CARL A. TREXLER

DECEMBER 1988

U.S. ARMY LABORATORY COMMAND

BALLISTIC RESEARCH LABORATORY

ABERDEEN PROVING GROUND, MARYLAND

DESTRUCTION NOTICE

Destroy this report when it is no longer needed. DO NOT return it to the originator.

Additional copies of this report may be obtained from the National Technical Information Service, U.S. Department of Commerce, Springfield, VA 22161.

The findings of this report are not to be construed as an official Department of the Army position, unless so designated by other authorized documents.

The use of trade names or manufacturers' names in this report does not constitute indorsement of any commercial product.

UNCLASSIFIED
SECURITY CLASSIFICATION OF THIS PAGE

REPORT DOCUMENTATION PAGE

Form Approved
OMB No. 0704-0188

1a. REPORT SECURITY CLASSIFICATION UNCLASSIFIED	1b. RESTRICTIVE MARKINGS
2a. SECURITY CLASSIFICATION AUTHORITY	3. DISTRIBUTION/AVAILABILITY OF REPORT Approved for public release; distribution is unlimited.
2b. DECLASSIFICATION/DOWNGRADING SCHEDULE	
4. PERFORMING ORGANIZATION REPORT NUMBER(S) BRL-MR-3725	5. MONITORING ORGANIZATION REPORT NUMBER(S)
6a. NAME OF PERFORMING ORGANIZATION U.S. Army Ballistic Research Laboratory 6b. OFFICE SYMBOL (If applicable) SLCBR-LF	7a. NAME OF MONITORING ORGANIZATION
6c. ADDRESS (City, State, and ZIP Code) Aberdeen Proving Ground, MD 21005-5066	7b. ADDRESS (City, State, and ZIP Code)
8a. NAME OF FUNDING/SPONSORING ORGANIZATION U.S. Army Ballistic Research Laboratory 8b. OFFICE SYMBOL (If applicable) SLCBR-DD-T	9. PROCUREMENT INSTRUMENT IDENTIFICATION NUMBER
8c. ADDRESS (City, State, and ZIP Code) Aberdeen Proving Ground, MD 21005-5066	10. SOURCE OF FUNDING NUMBERS PROGRAM ELEMENT NO. 62618A PROJECT NO. 1L1 62618AH80 TASK NO. WORK UNIT ACCESSION NO.

11. TITLE (Include Security Classification)
Pressure Measurements on the Interior Surface of a 75mm Tubular Projectile at Mach 4 (U)

12. PERSONAL AUTHOR(S)
Kayser, Lyle D.; Yalamanchili, Rao J.; and Trexler, Carl A. *

13a. TYPE OF REPORT	13b. TIME COVERED	14. DATE OF REPORT (Year, Month, Day)	15. PAGE COUNT
Memorandum Report	FROM _____ TO _____	1988 October	35

16. SUPPLEMENTARY NOTATION
* NASA Langley Research Center, Hampton, VA 23665

17. COSATI CODES		
FIELD	GROUP	SUB-GROUP
01	01	

18. SUBJECT TERMS (Continue on reverse if necessary and identify by block number)
Projectiles
Tubular Projectiles;
Internal Pressures
Ramjets;

19. ABSTRACT (Continue on reverse if necessary and identify by block number)

Wind tunnel pressure measurements were obtained on the interior surface of a solid-fuel-ramjet, tank-gun, training projectile. All data were obtained at Mach 4.03, a free-stream Reynolds number of approximately 76.6×10^6 per meter and at zero degrees angle of attack. The tests were preliminary in nature and were not intended to simulate actual flight conditions. The projectile was not spinning and there was no burning of fuel nor was there any simulated burning by gas injection. The injector hole diameter, upstream from the fuel section, was varied and some injectors were notched to form vortex generators. Two conventional nozzles were tested and a third nozzle was equipped with a butterfly valve so that pressure distributions could be obtained at various levels of flow restriction. Schlieren photography was available to help determine if the flow was choked by showing an attached or detached shock at the inlet leading edge. Some apparent critical flow behavior is indicated by drastic changes in pressure distribution for modest changes in internal geometry.

20. DISTRIBUTION/AVAILABILITY OF ABSTRACT	21. ABSTRACT SECURITY CLASSIFICATION
☐ UNCLASSIFIED/UNLIMITED ☒ SAME AS RPT. ☐ DTIC USERS	UNCLASSIFIED
22a. NAME OF RESPONSIBLE INDIVIDUAL Lyle D. Kayser	22b TELEPHONE (Include Area Code) (301)-278-3815 22c. OFFICE SYMBOL SLCBR-LF-A

DD Form 1473, JUN 86 *Previous editions are obsolete.*

SECURITY CLASSIFICATION OF THIS PAGE
UNCLASSIFIED

Table of Contents

List of Tables

List of Figures

I. Introduction

A program to develop a solid-fuel, tubular projectile as a training munition for tank launched armor piercing projectiles has been underway at the U.S. Army Ballistic Research Laboratory (BRL) in conjunction with the U.S. Army Chemical Research and Development Engineering Laboratory and the Chemical Systems Division of the United Technologies Corporation by contractual agreement. The goal of the program is to demonstrate a tank gun training round (TGTR) of low dispersion at three kilometers and, for safety, a maximum range of eight kilometers. References 1, 2, 3, and 4 describe some of the development phases of the TGTR and document results of free-flight trajectories where projectiles were tracked with Hawk (doppler) radar and smear photographs were obtained near the muzzle to verify ignition and sabot separation characteristics.

The concept of the TGTR is to use thrust of a solid fuel ramjet to decrease total drag and obtain a ballistic match with low drag, armor piercing tank munitions for ranges up to three kilometers. When the solid propellant is depleted, the velocity steadily decays until flow through the projectile is choked or partially choked and the projectile effectively becomes a blunt-body high-drag configuration which will not fly more than eight kilometers horizontal range.

To support the TGTR development program, a wind tunnel test program has been initiated. The wind tunnel program is being carried out in a cooperative effort by the BRL and the Hypersonic Propulsion Branch, High Speed Aerodynamics Division, NASA Langley Research Center. The initial phase of wind tunnel testing is to obtain internal surface pressure measurements on a nonspinning projectile with no burning or simulation of burning. The initial phase is not expected to provide design parameters for a TGTR, but it should provide some basic understanding of the internal flow as well as a data base for verification of computational codes. Computational efforts for the simple cold flow will be carried out and verified before the more complex simulations involving spin and burning are attempted.

Computational efforts for internal flows have been underway at the BRL in recent years. Nietubicz and Heavey[5] has applied an unsteady, thin-layer Navier-Stokes code to a spinning tubular projectile and to a ramjet type configuration. More recently, Nusca

[1] *Mermagen, W.H. and Yalamanchili, R.J., "Experimental Tests of a 105/75mm Solid Fuel Ramjet Tubular Projectile," US Army Ballistic Research Laboratory, Aberdeen Proving Ground, Maryland, BRL-MR-03416, December 1984. (AD B089766)*

[2] *Mermagen, W.H. and Yalamanchili, R.J., "First Diagnostic Tests of a 75mm Solid Fuel Ramjet Tubular Projectile," US Army Ballistic Research Laboratory, Aberdeen Proving Ground, MD, BRL-MR-03282, June 1983. (AD A130598)*

[3] *Olson, D. and Mermagen, W.H., "Initial Test Firings of a Solid Fuel Ramjet Tubular Projectile,"US Army Ballistic Research Laboratory, Aberdeen Proving Ground, MD, BRL-MR-03212, November 1982. (AD B069824L)*

[4] *Olson, D. and Mermagen, W.H., "Demonstration Test Firings of a Solid Fuel Ramjet Tubular Projectile," US Army Ballistic Research Laboratory, Aberdeen Proving Ground, MD, BRL-MR-03213, November 1982. (AD B069823L)*

[5] *Nietubicz, C.J., and Heavey, K.R., "Computational Flow Predictions for Ramjet and Tubular Projectiles," Proceedings of the Eighth International Symposium on Ballistics, Orlando, Florida, October, 1984.*

et al [6] applied a Navier-Stokes code with a class of algorithms termed 'total variational diminishing' (TVD) to the TGTR configuration. Danberg and Sigal [7] have analyzed the different types of internal flow behavior and have provided an axisymmetric method of characteristics solution which was compared to computational results.

II. Experiment

1. Model

The basic model geometry is shown in Figure 1. The model is seen to have a divergent inlet up to 73.7mm where an injector is located. A mock fuel grain of 140.7mm length is located from the injector to the nozzle inlet. A convergent-divergent nozzle is located in the final 50.8mm of the projectile. The nozzle, mock fuel grain, and injector were removable from the rear of the model so that internal configuration changes could be made. The geometry of the various injectors is shown in Figure 2. Two conventional nozzles with throat diameters of 39.1mm (basic configuration) and 40.9mm were tested. The larger 40.9mm nozzle was made to accommodate a butterfly valve which can be seen in the model rear view of Figure 3. The butterfly pivots at the nozzle throat and when it is in the fully opened position, the open throat area equals that of the 39.1mm nozzle. The butterfly control rod was driven by a motor-gear system equipped with a potentiometer which provided an output proportional to the angular motion of the rod.

The model was instrumented with 23 pressure ports with openings to the model interior and positioned at axial location listed in Table 1. The model shell is very thin and it was nearly impossible to imbed the pressure tubing in the model wall, so the tubing was positioned on the exterior surface as shown in Figure 4. Since the free-stream flow was always to be fully supersonic, the external disturbances caused by the tubing should not affect the interior flow. The pressure tubing used was monel with an OD of 1.59mm and an ID of 1.09mm. Since the mock fuel grain and the nozzles were removable, O-ring seals were used to prevent pressure propagation along the interface between the inserts and the model shell. Figure 5 shows the two nozzles and the mock fuel grain with the O-rings installed.

2. Test Facilities

The model was tested in the Mach 4, nine inch blowdown tunnel, at the NASA Langley Research Center. The wind tunnel has a two-dimensional fixed nozzle with a calibrated Mach number of 4.03 and a 229 x 229mm test section. Stagnation pressures range from 12 to 15 atmospheres (standard sea level) and stagnation temperatures are approximately 285K; these stagnation conditions give test section Reynolds numbers of

[6] *Nusca, M., Chakravarthy, S., and Goldberg, U., "Computational Fluid Dynamics Capability for Solid Fuel Ramjet Projectiles," US Army Ballistic Research Laboratory, Aberdeen Proving Ground, BRL-MR in preparation.*

[7] *Danberg, J.E., and Sigal, A., "Evaluation of Solid Fuel Ramjet Projectile Aerodynamic Characteristics," Proceedings of the 10th International Symposium on Ballistics, Vol I, San Diego, California, october 1987.*

about (65–80)x10^{-6} based on a length of one meter. The tunnel is vented to the atmosphere, which prevents operation of the tunnel at low stagnation pressures and therefore at low Reynolds number conditions. The tunnel is equipped with a Schlieren system which includes 0.28 meter diameter optical windows. A Schlieren screen can be monitored during a test and Schlieren images can be recorded on film. The model pressure tubing was connected to a Pressure Systems Inc., 64 channel Electric Scanning Pressure system. All channels were calibrated for a range of 0 to 3 atmospheres compared to a measurement range of 0 to 2 atmospheres. A MOD COMP IV-35 mini-computer provided control of the data acquisition. Data can be recorded up to 10 times per second on magnetic tape for subsequent processing. A quick look capability is available that provides 40 scans (cycles) of tabulated and plotted data.

3. Procedure

Table 2 is a summary of all wind tunnel tests up to September 30, 1985. The test data are identified by run numbers, batch numbers, and cycle numbers. While the tunnel is running, all data channels are scanned at specified intervals (e.g. 1.0 sec intervals) and the cycle number is incremented for each scan. The procedure for the conventional nozzles was to start the tunnel and record data for 30-40 seconds at one second intervals. Pressures stabilized quickly and there was no significant change in the data for successive scans (cycles). For the butterfly nozzle tests, the tunnel was started with the valve in the open position, then the valve was cycled in small increments to the closed position and then back to the open position. Since substantial pressure changes occurred, 120 seconds of data (quick look) at three second intervals were recorded. All data were recorded on magnetic tape at five samples per second for post processing

Leak checks prior to the start of testing indicated leak rates on the order of 10^{-4} atm over a 60 sec time span at low pressures. Since pressure stabilization times were on the order of one second, it is believed that leakage was generally not a problem. When nozzles were removed from the model, sometimes minor cuts were observed on the small O-rings, (see Figure 5) which may have permitted leakage to the nozzle transducers, however, no problem was observed with the larger circumferential O-rings. Atmospheric pressure measurements were made by all pressure channels periodically through out the tests–pressures were within 0.5 percent of the mean value. Comparisons of adjacent pressures at several pressure levels, and at certain conditions, showed consistent behavior and provided additional assurance of good quality measurements.

III. Results

Plotted results are presented in Figures 6-17 and a tabulation of the data are given in Tables 3 to 8. Tables 3 to 6 are for the conventional nozzles and for the nozzle with the fully opened butterfly valve. Tables 7 and 8 give a limited amount of data which show the effects of rotating the butterfly valve from the fully opened to the fully closed positions.

Figures 6, 7, and 8 show the effects of varying the hole size in the injectors for the

three nozzle configurations. Figure 6, 39.1mm nozzle data, shows three distinct curves for the three different injectors. Subsequent comparisons of data and analyses will illustrate that the three different curves correspond to three distinct classes, or modes, of internal flow. Generally, depending on the internal geometry, the flow will lock in to one of these modes and changes between these modes occur in a discontinuous manner. For purposes of discussion the three modes are defined as follows: Mode 1 (supersonic inlet), the inlet pressures are constant and on the order of 0.8 to 1.0 times free stream static pressure (p_∞) as seen for the 48.3mm injector; Mode 2 (Weak shock compression), the inlet pressures are constant and on the order of four times (p_∞) as seen for the 43.2mm injector; Mode 3 - (Strong shock compression), the highest, and non-constant inlet pressures as those seen for the 38.1mm injector of Figure 6. Flow for these three modes is believed to be fully swallowed at the inlet. No spillage or decrease in mass flow through the projectile model occurs.

Figure 7 show data for the nozzle with the butterfly valve and for the same injectors. The nozzle open area is the same as that for the 39.1mm nozzle but comparisons with Figure 6 show substantial differences for two of the injectors. Pressures for the 48.3mm injector have increased from one to four times (p_∞) which indicates a change from the mode 1 to the mode 2 case. Also, the pressures are very nearly equal to the mode 2 pressures of Figure 6 for the 39.1mm nozzle and the 43.2mm injector. Pressures for the 43.2mm injector have increased and are now indicative of mode 3 type flow. Pressures for the 38.1mm injector are virtually identical to those of Figure 6 which show that, for this case, the difference in nozzle geometry was not sufficient to change the flow mode.

Figure 8 shows data for the 40.9mm nozzle and the same injectors, but the throat area is approximately 9% larger than areas for the nozzles of Figures 6 and 7. Comparisons with Figure 7 show that flow for the 43.2mm and 48.3mm injectors jumps to the mode 1 type, and that flow for the 38.1mm injector remains at mode 3.

Figure 9 shows a quasi-stable occurrence where the flow has changed from mode 3 to mode 2 while the tunnel was running and no significant changes in tunnel conditions were being made. This is the same configuration as that of Figure 6 for the 43.2mm injector. Repeat runs indicated that mode 2 was dominant and mode 2 data was therefore presented in Figure 6.

Figures 10 to 13 show data for the vortex generator injectors. The generator with a 3.8mm step has an open area very close to that of the 43.2mm injector; an equivalent diameter, based on the open area, for this generator is 43.1 mm. The equivalent diameter for the generator with a 6.4mm step is 41.3 mm and is, therefore, between that of the 38.1mm and the 43.2mm injectors. Elements for one of the generators with a 3.8mm were slightly twisted. As will be shown, this generator sometimes produces a mode change in the flow. Comparison of Figures 10 and 11 shows a remarkable agreement of the vortex generator data with th 39.1mm and the butterfly nozzles. The only slight differences in pressure that can be detected are in the nozzle area. This data would seem to show that the butterfly disk did not affect the results. However, as shown above in Figures 6 and 7, the butterfly changed the flow mode for two of the circular injectors.

Figure 12 shows pressures for the vortex generators for the slightly larger 40.9mm

nozzle. Apparently, the momentum loss for vortex generator with twisted elements is less than that for the other generators, and combined with the slightly larger nozzle, the flow jumps from a mode 3 flow to a mode 1 type flow. The other two generators remain at the mode 3 type flow but the pressure levels are slightly less than for the other two nozzles as seen in Figures 10 and 11.

Figure 13 shows a quasi-stable occurrence for the vortex generator with twisted elements when tested in conjunction with the 39.1mm nozzle. During a test run, flow jumped from a mode 3 type to a mode 1 type for no apparent reason. The run was repeated and the flow remained at the higher pressure mode 3 for the entire run. This seemed to indicate a dominance toward mode 3, and was, therefore, presented in Figure 10 rather mode 1 data.

The effects of rotating the butterfly valve on the longitudinal pressure distribution are illustrated in Figure 14. With the valve fully open (zero deg), the pressures agree with the mode 3 type which were show in Figure 7. As the valve is rotated, the level of pressure rises; but at 31 degrees, the flow still exhibits a mode 3 type behavior. As the valve is rotated further to 38 and 41 degrees, the inlet pressures change character and are seen to increase which would be indicative of a subsonic flow. Pressure levels reached a maximum at about 57 degrees and for practical purposes, the flow is fully choked for angles of 57 to 90 degrees. The pressure levels do not quite attain the the theoretical level of that behind the normal shock (p_{t2}) which might be expected since the butterfly does not fully block the nozzle throat.

The effect of rotating the butterfly on selected pressures is shown in Figure 15 – pressure taps 1,5,8,10 are in the inlet area and pressure taps 15 and 19 are in the fuel section. The steep pressure rise in the area of 35 to 40 degrees indicates transition from the mode 3 type flow to a subsonic or choked flow. The character of the choked flow is seen to be distinct from that of modes 1,2, and 3 and is therefore designated as a mode 4 type flow.

Figures 16 and 17 compare pressures for runs that were obtained on different dates and demonstrate good repeatability. Duplicate runs were made on several other occasions, and also showed good repeatability. Absolute pressures levels were checked by comparing choked flow values to theoretical values of pressure behind a normal shock. Also, air-off pressures were frequently compared to atmospheric barometer readings. These various checks provide assurance that the pressure measurements were of good quality.

IV. Discussion

At the time the data were acquired, no flow model or computational results existed which would help describe the physics of the internal flow from which the pressure data were obtained. Nietubicz[5] obtained internal flow for two different geometries, but neither geometry was sufficiently close to that of Figure 10 that comparisons to the experiment could be made. Cursory analyses of the experimental results did provide sufficient insight to the flow behavior and the conclusions were only partially correct. Because of the low

pressures encountered in the mode 1 type flow, it was believed that flow through the inlet and fuel section was predominantly supersonic. It seemed fairly obvious that the higher pressures levels of Figures 14 and 15 were indicative of choked (mode 4) type flow. The mode 2 and mode 3 type flows were more difficult to understand, but it was deduced that the inlet flow must be compressed through an oblique shock in order to achieve levels of 4-8 times the free-stream static pressure. It was further estimated that subsequent rises in pressure in the inlet or in the fuel section of up to 10 times the free-stream static pressure were too low to indicate subsonic flow. Therefore, the conclusion was made that flow through the inlet and fuel sections was predominantly supersonic – no distinction was made between the mode 2 and mode 3 type flows.

Recent computations by Nusca[6] and Nietubicz were in agreement with the mode 1 type flow. Their results show that flow through the core is supersonic and that a separation regions exist along the wall between the inlet leading edge and the injector step and between the injector step and the nozzle. Nusca also computed the flow for nozzles with a smaller throat diameter which resulted in choking of the flow. These results were similar to those of Figure 8a where choking was induced by the butterfly valve at about 44 degrees.

Danberg[7] found that mode 2 flow, which shows a nearly constant pressure in the inlet, can be interpreted as a flow produced by an over-expanded jet. He provided an axisymmetric method of characteristics solution for the inlet region with the assumption that jet exit (which corresponds to the TGTR inlet) pressure was four times the free-stream static pressure. This predicted flow field was compared to numerical computational results by Patel (unpublished results shown in reference 7) which predicted the mode 2 inlet pressure of four times the free stream static pressure (p_∞), and was found to be in good agreement. For the jet flowing into the inlet at four times (p_∞), an oblique shock emanating from the inlet lip provides the mechanism for the required pressure rise. The oblique shock turns the flow towards the centerline. As it focuses toward the centerline, it is terminated by the formation of a normal shock disc. A second oblique shock is required to turn the flow parallel to the centerline. The jet boundary, or free-streamline, emanates from the inlet lip and leaves a dead air, or separated, region between the free streamline and the inlet cowl. Van Dyke [8] presents a photograph of such a jet which is believed to be a good qualitative representation of the mode 2 inlet flow. A small region of subsonic flow would have to exist just behind the normal shock disk, but expansion waves accelerate the flow. The overall flow is predominantly supersonic.

Danberg has found that the mode 3 flow, where the higher inlet pressure decreases and then increases, can be can be explained by the existence of a strong oblique shock wave (from the strong shock solution) which stands just inside the inlet. A small region of high subsonic flow must exist behind the shock wave, but the decreasing pressure suggests an expansion to supersonic flow. As the flow moves towards the injector step, the pressure rise indicates the existence of a shock wave which may emanate from a separated region ahead of the injector step. The pressure drop just downstream from the injector, as shown in Figures 10, 11, and 12, is consistent with that of an expanding supersonic flow. A supersonic flow moving towards the nozzle throat, which is smaller in area, would have to decelerate and one dimensional analysis would predict a pressure increase. This pressure

[8] *Milton van Dyke, "An Album of Fluid Motion," Plate no.168, Parabolic Press.*

rise in the fuel section is characteristic of both the mode 2 and mode 3 type flows.

Figure 14 shows that for butterfly angles of approximately 0-31 degrees, the pressure levels change but still indicate the mode 3 characteristics. For angles of 38 degrees and larger, pressures levels increase but are now characteristic of a choked flow. The changes in the character of the flow occur in a gradual manner as opposed to the abrupt changes which occur between modes 1,2, and 3.

It was generally found that increasing the internal blockage by decreasing the injector diameter or the nozzle throat diameter, forced the flow towards a higher mode (mode 1 is supersonic and mode 4 is choked). The vortex generators provided more effective blockage, based on the open area, than the injectors with circular holes. The vortex generators with 3.8mm and 6.4mm steps and equivalent diameters of43.1mm and 41.3mm, respectively, gave pressure distributions very close to those for the 38.1mm circular injector. The effectiveness of the injector with a 3.8mm twisted step and a 43.1 mm effective diameter seemed to fall between that of the 38.1mm and the 43.2mm circular injectors.

The flow conditions for these cold flow tests are not expected to be similar to those in flight with burning propellant. The critical behavior and mode changes observed in these tests would not likely be encountered during flight. The tests did provide results for complex flow fields which were interesting but difficult to analyze, and the results have provided significant challenges to CFD simulations.

V. Conclusions

1. Various pressure checks provide assurance that measurements are of good quality.
2. The data are interpreted to show the following distinct types of flow:
   A. Mode 1; Fully supersonic core flow.
   B. Mode 2; Weak shock inlet compression, predominantly supersonic, swallowed flow.
   C. Mode 3; Strong shock inlet compression, predominantly supersonic, swallowed flow.
   D. Mode 4, Choked flow with butterfly valve blockage.
3. Changes in the flow between modes 1,2, and 3 occur in a discontinuous manner. Change from mode 3 to mode 4 type flow occurs gradually.
4. Some of the internal geometries were near a critical state since mode changes occurred for little or no change in geometry.
5. The model configuration selected for these tests is considered to be a useful choice, though flight parameters were not closely simulated. The test results demonstrated complex flow fields which provide valuable and challenging tests for CFD simulations.

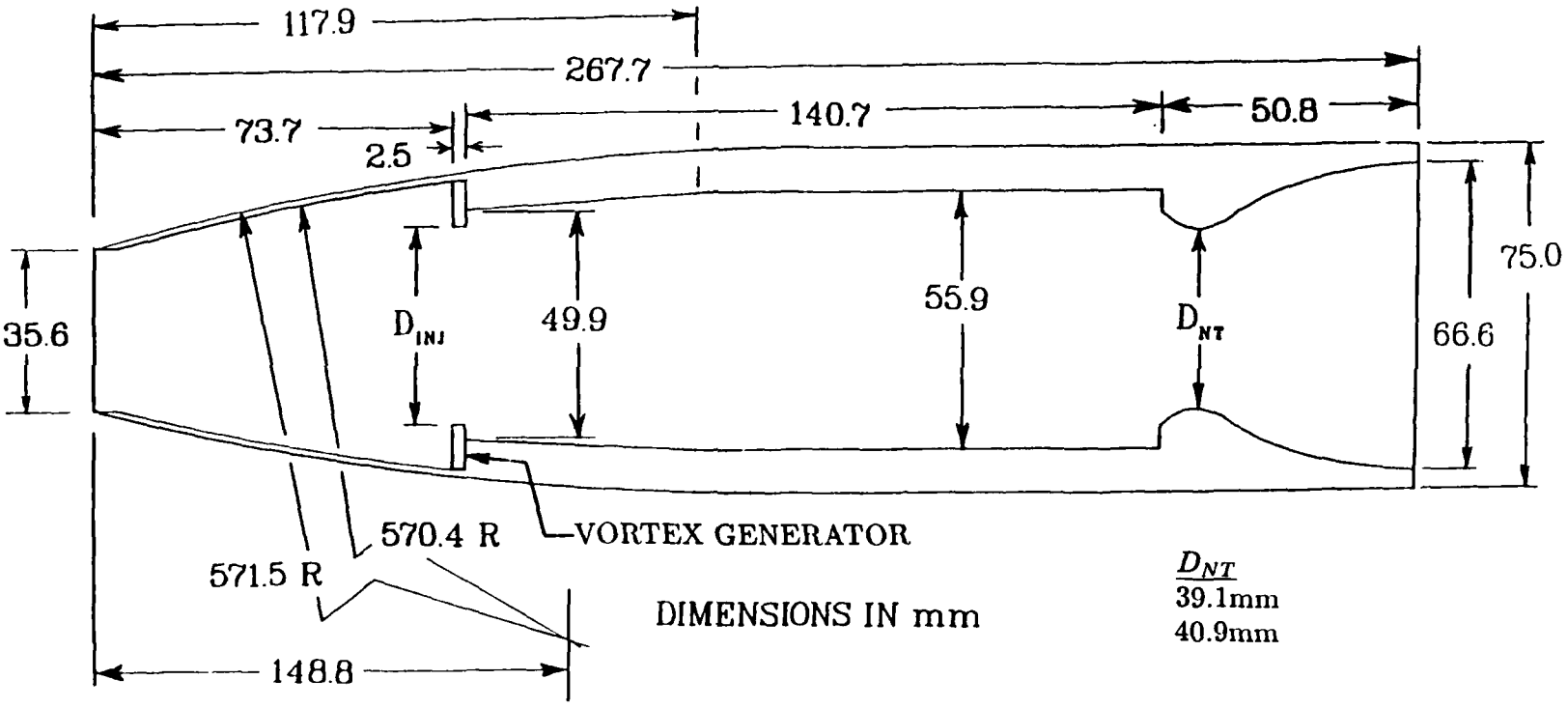

Figure 1. Model geometry

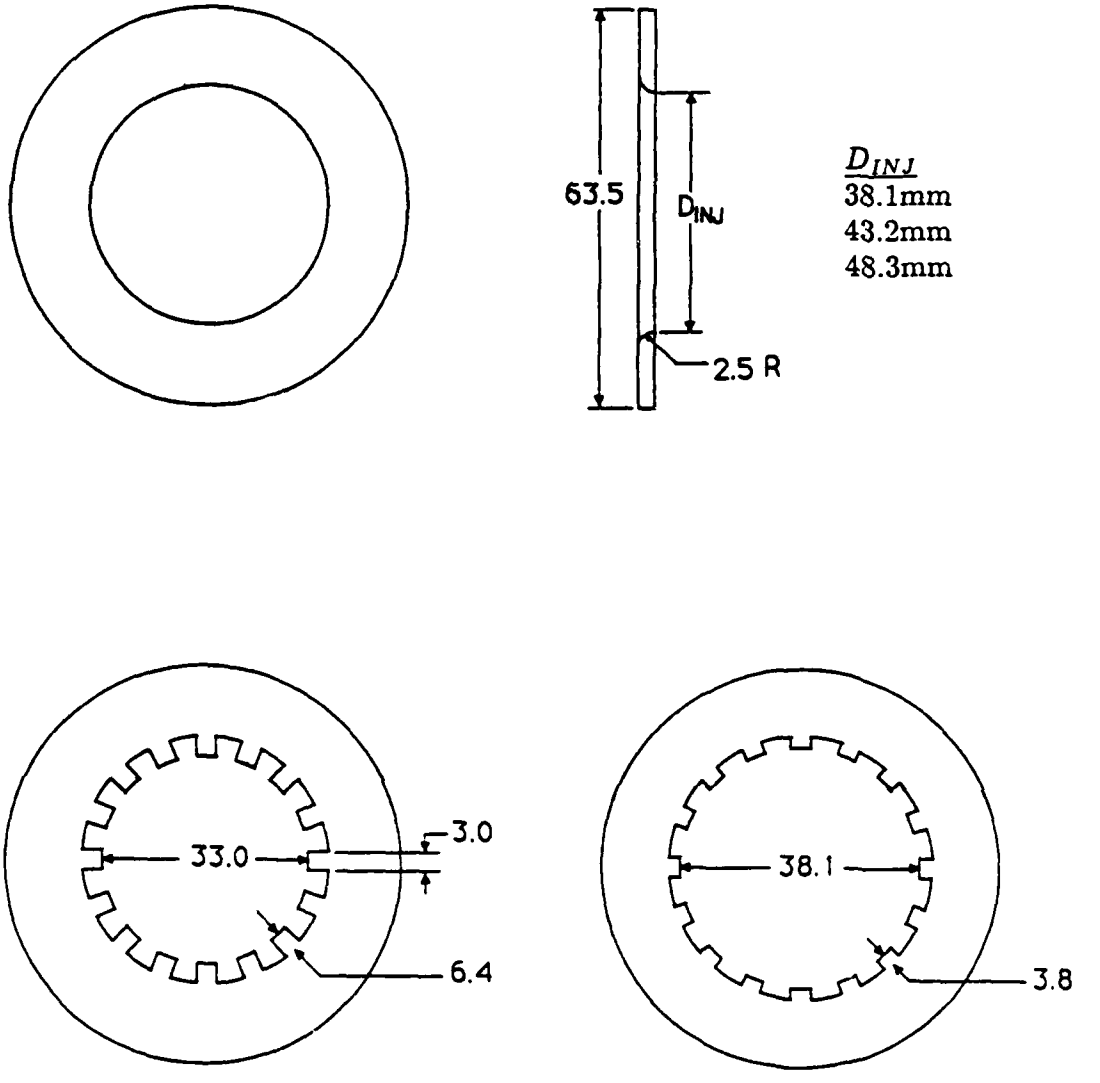

VORTEX GEN, 6.4mm step
$\bar{D}_{INJ} = 41.3mm$

VORTEX GEN, 3.8mm step
VORTEX GEN, 3.8mm step w/twist
$\bar{D}_{INJ} = 43.1mm$

all dimensions in mm

Figure 2. Injector geometries

Figure 3. Photograph of nozzle with butterfly valve

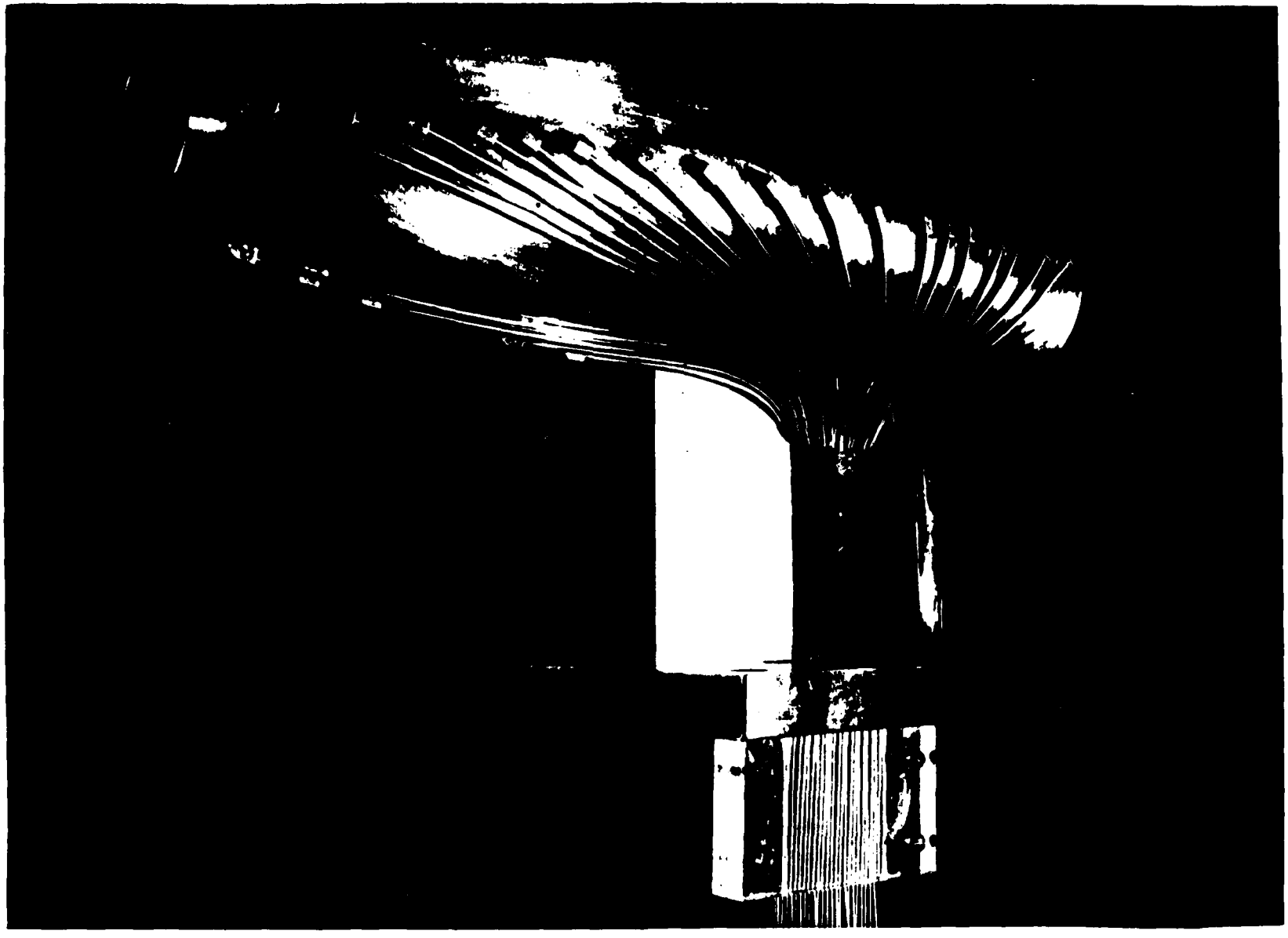

Figure 4. Model photograph showing external tubing

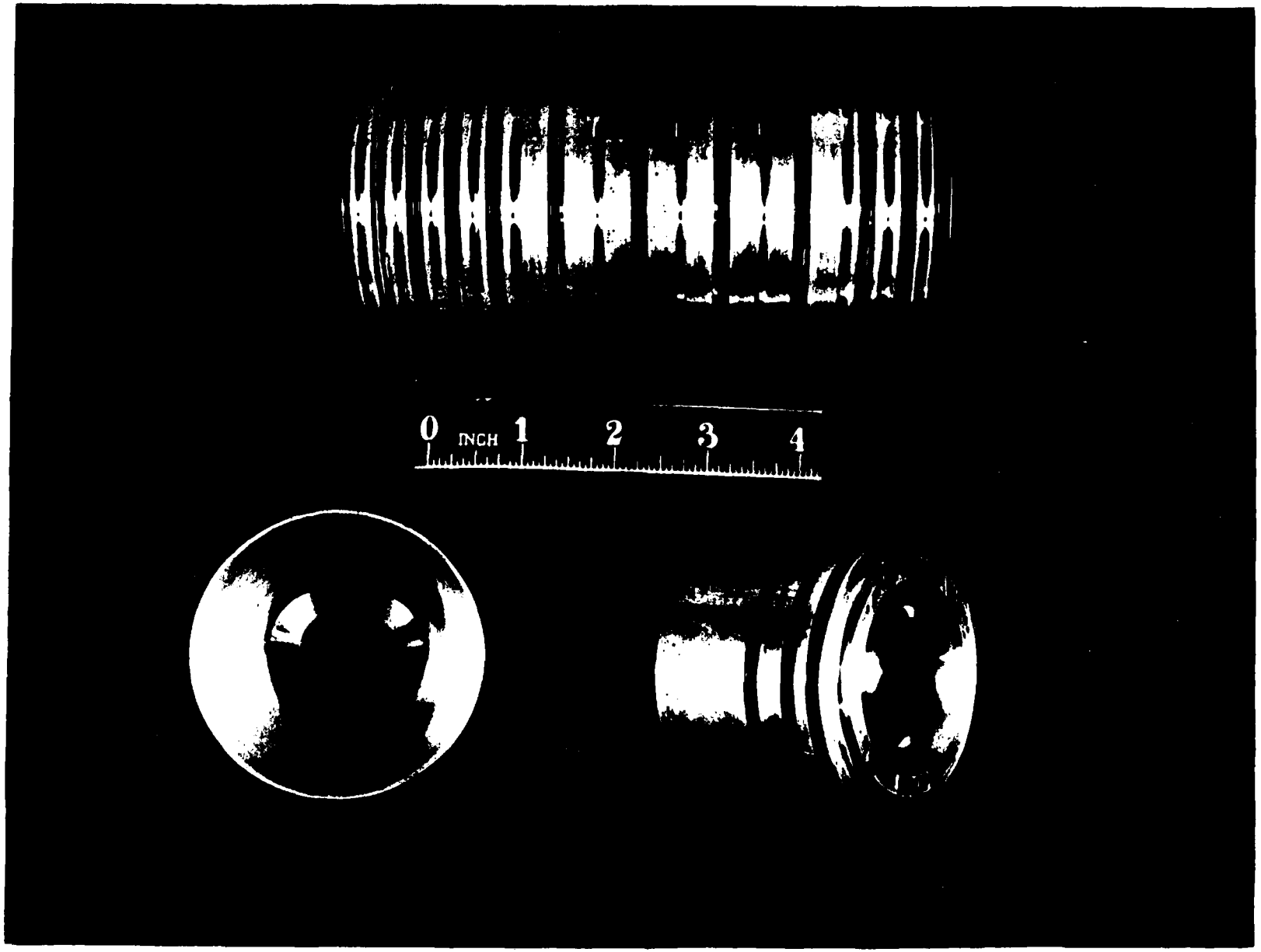

Figure 5. Nozzles and mock fuel grain photograph

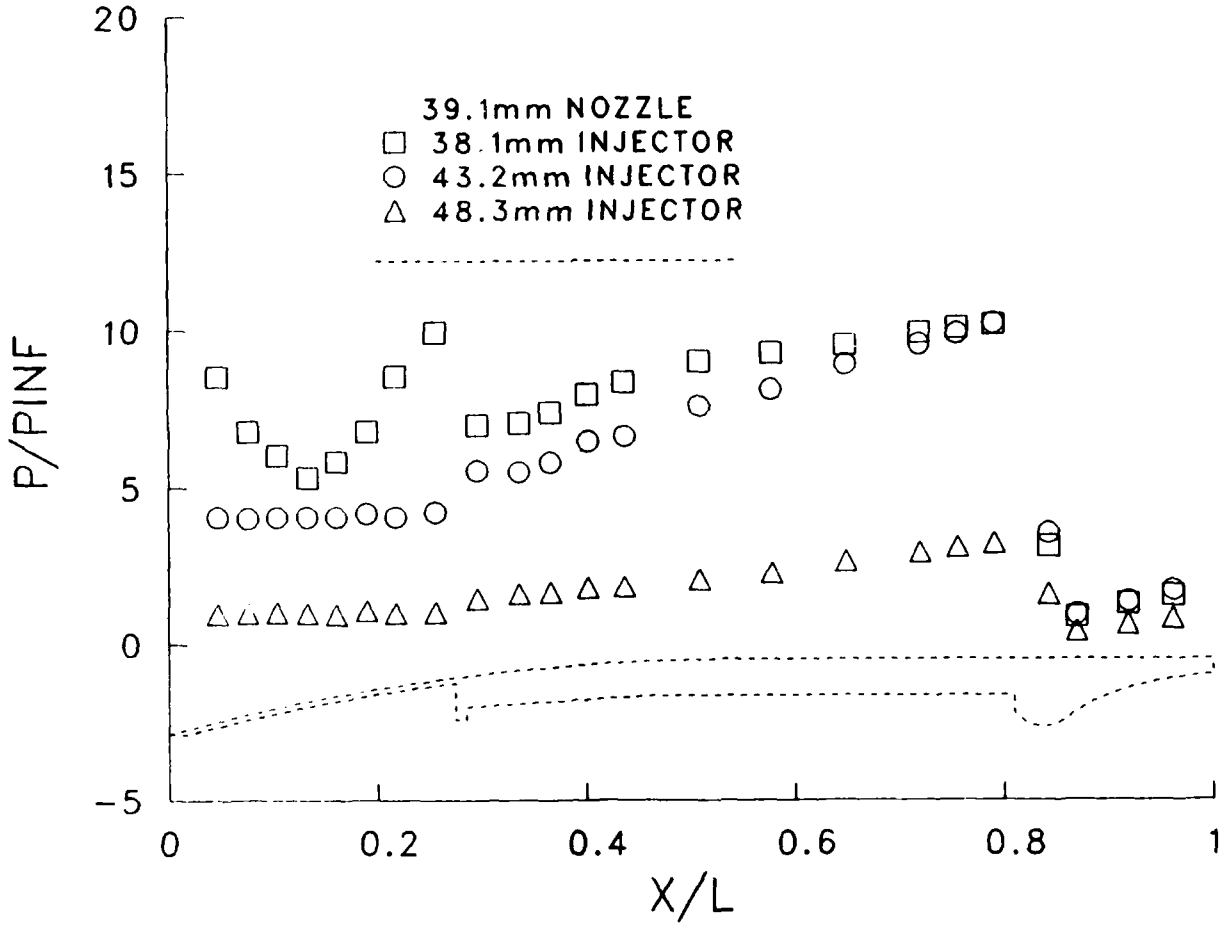

Figure 6. Effect of injector hole diameter - 39.1mm nozzle

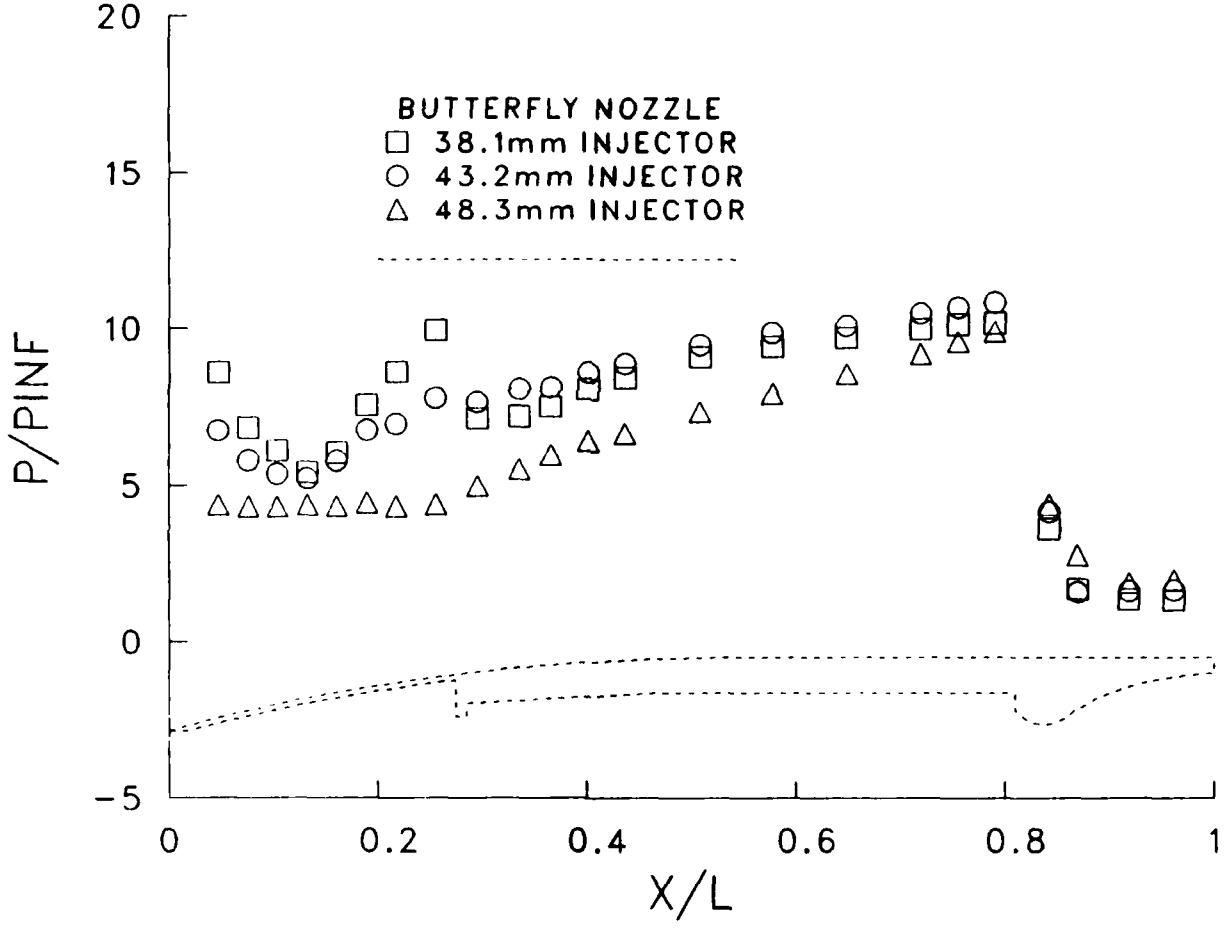

Figure 7. Effect of injector hole diameter - nozzle w/butterfly open

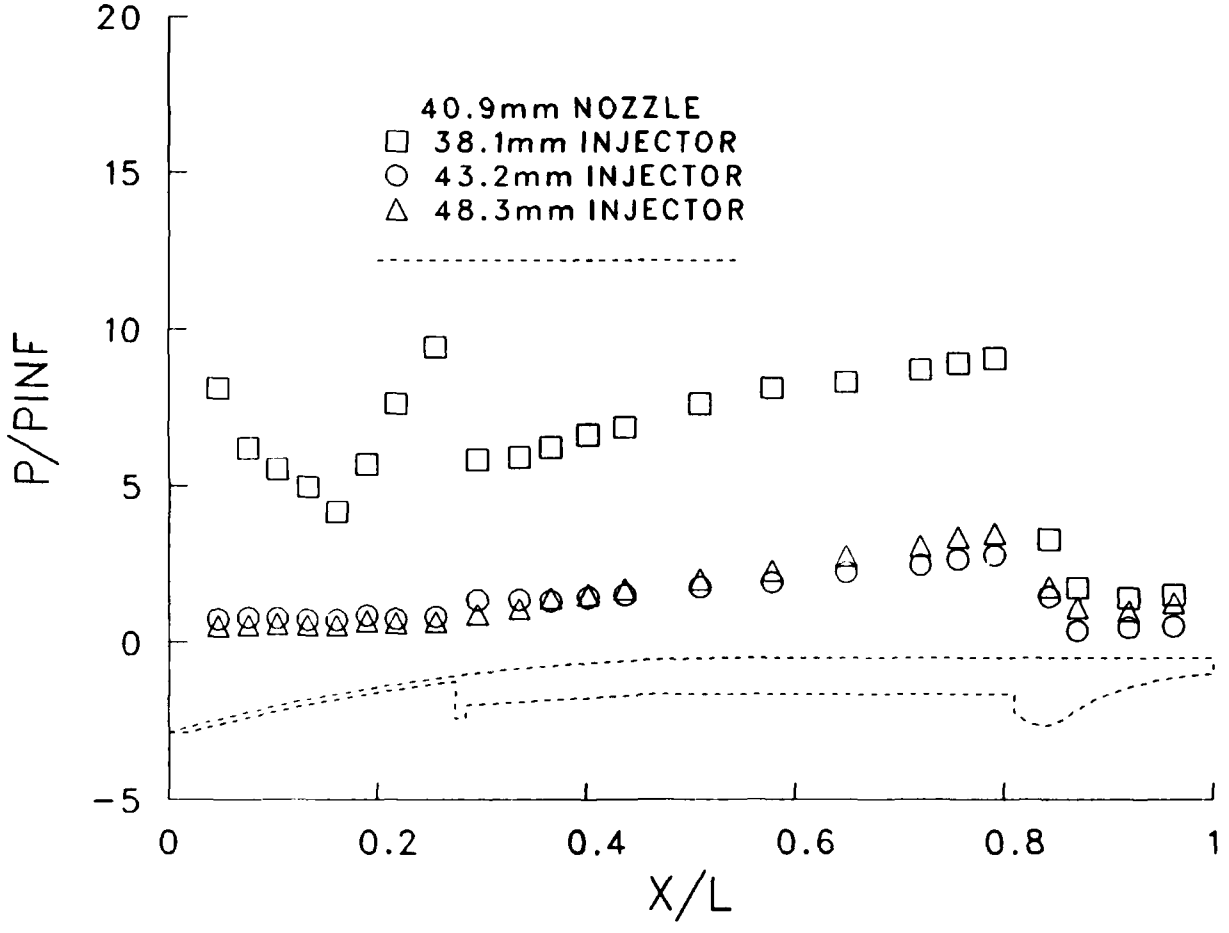

Figure 8. Effect of injector hole diameter - 40.9mm nozzle

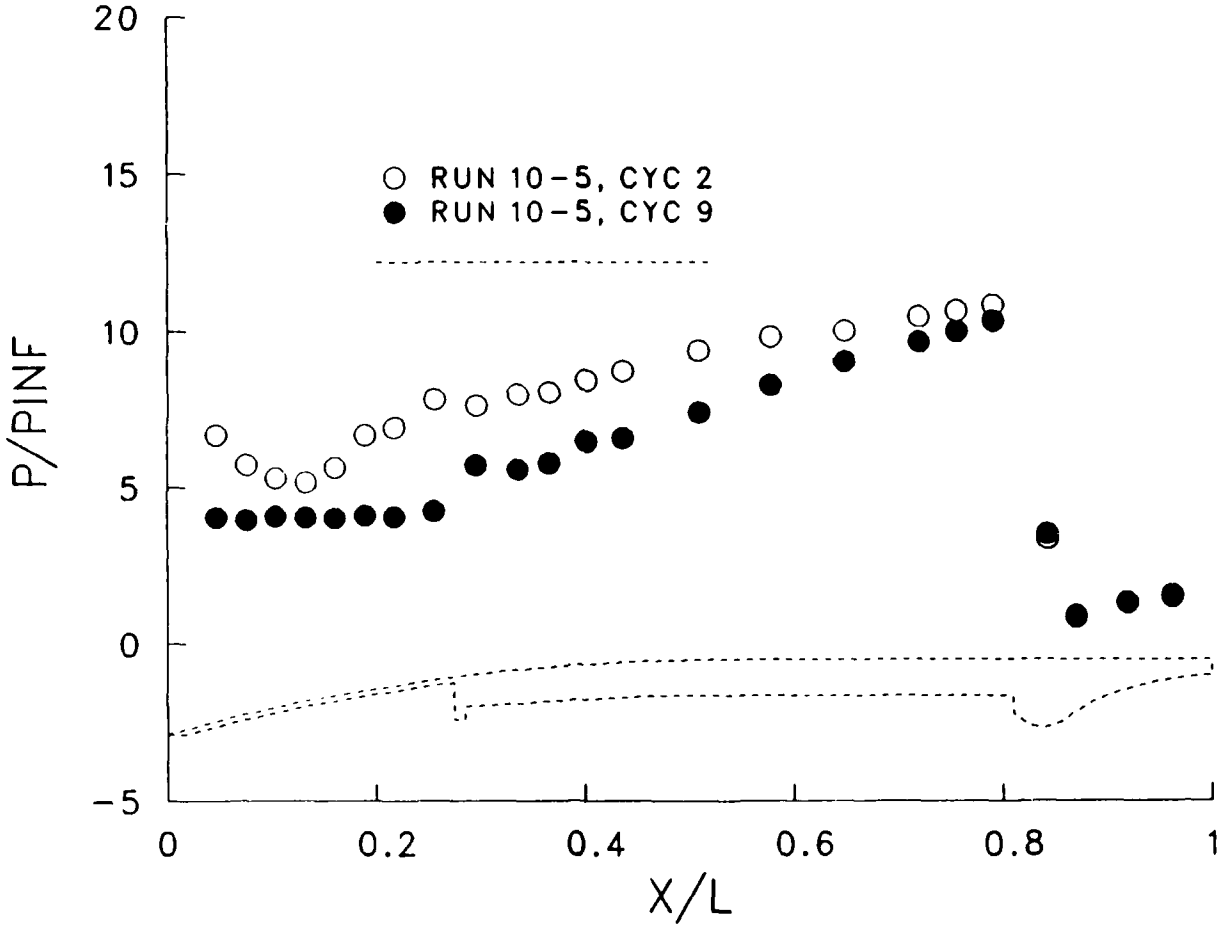

Figure 9. Quasi-stable occurrence, 39.1mm nozzle, 43.2mm injector

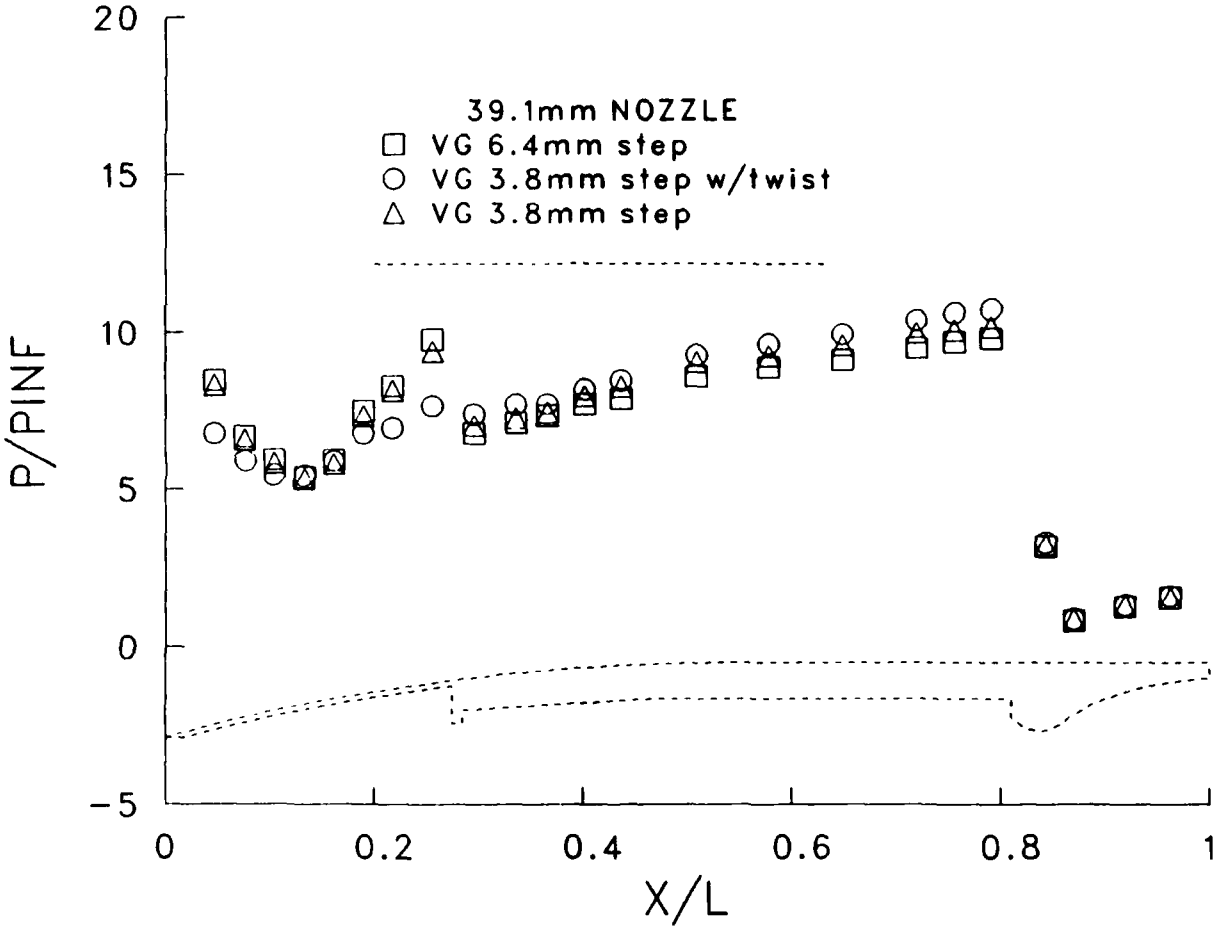

Figure 10. Effect of vortex generator geometry - 39.1mm nozzle

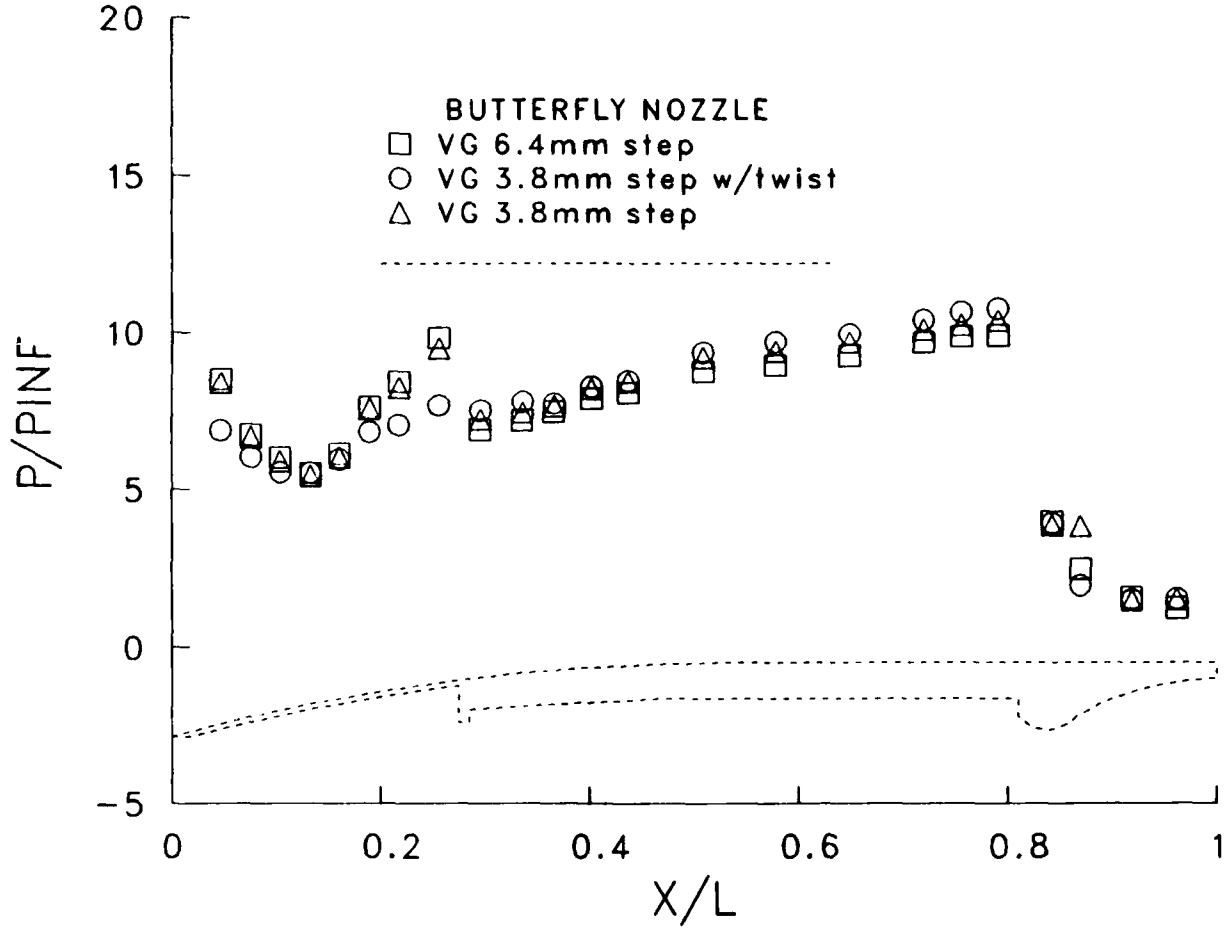

Figure 11. Effect of vortex generator geometry - nozzle w/butterfly open

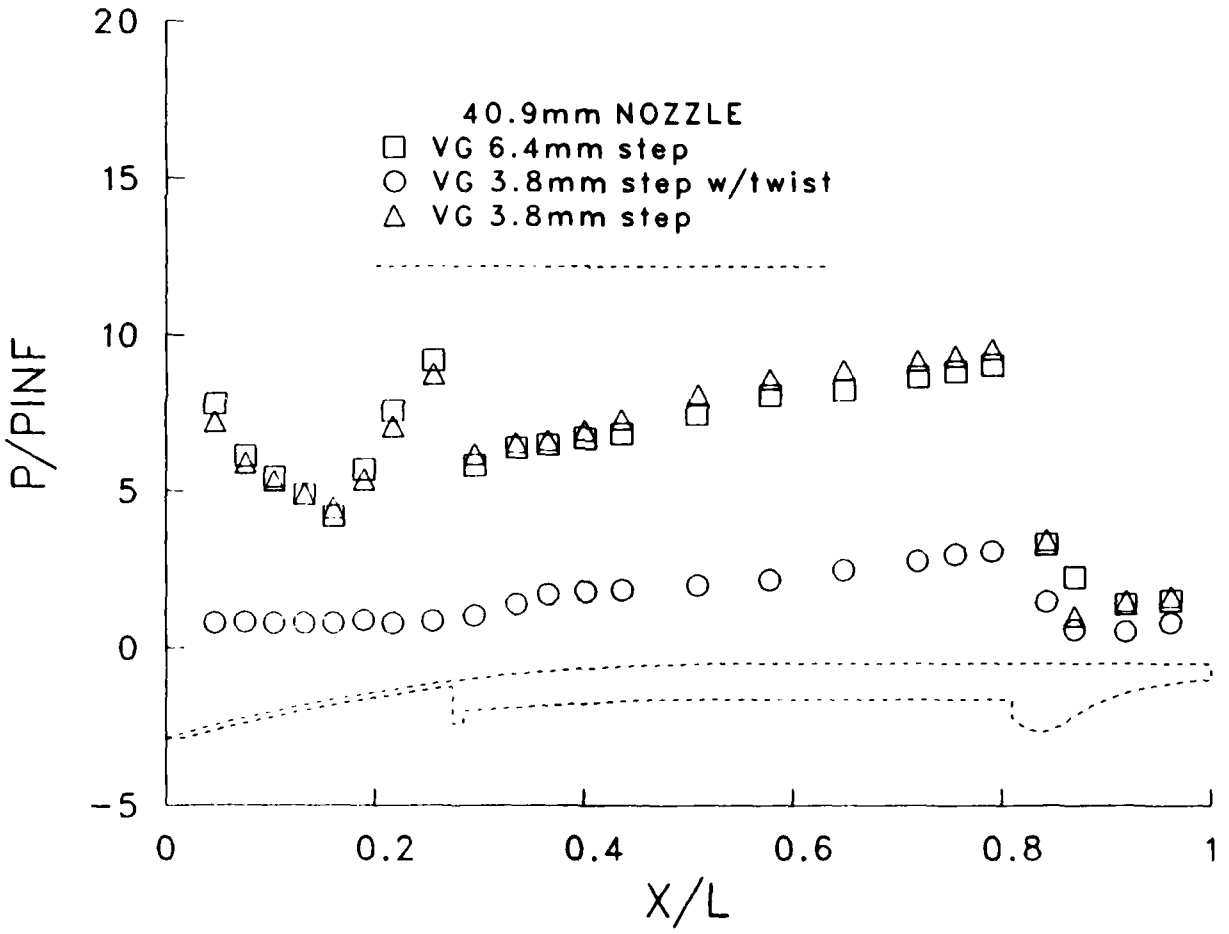

Figure 12. Effect of vortex generator geometry - 40.9mm nozzle

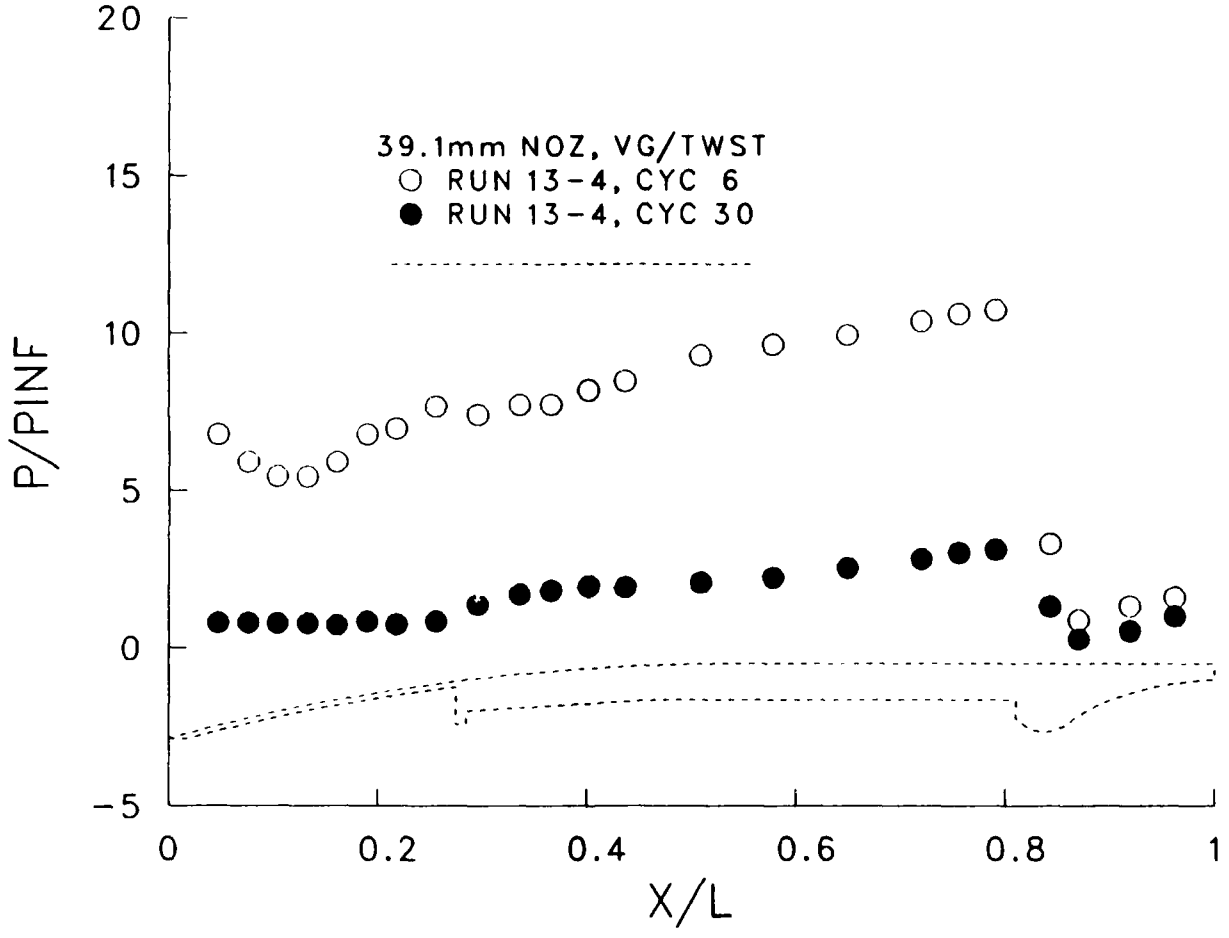

Figure 13. Quasi-stable occurrence, 39.1mm nozzle, vortex generator

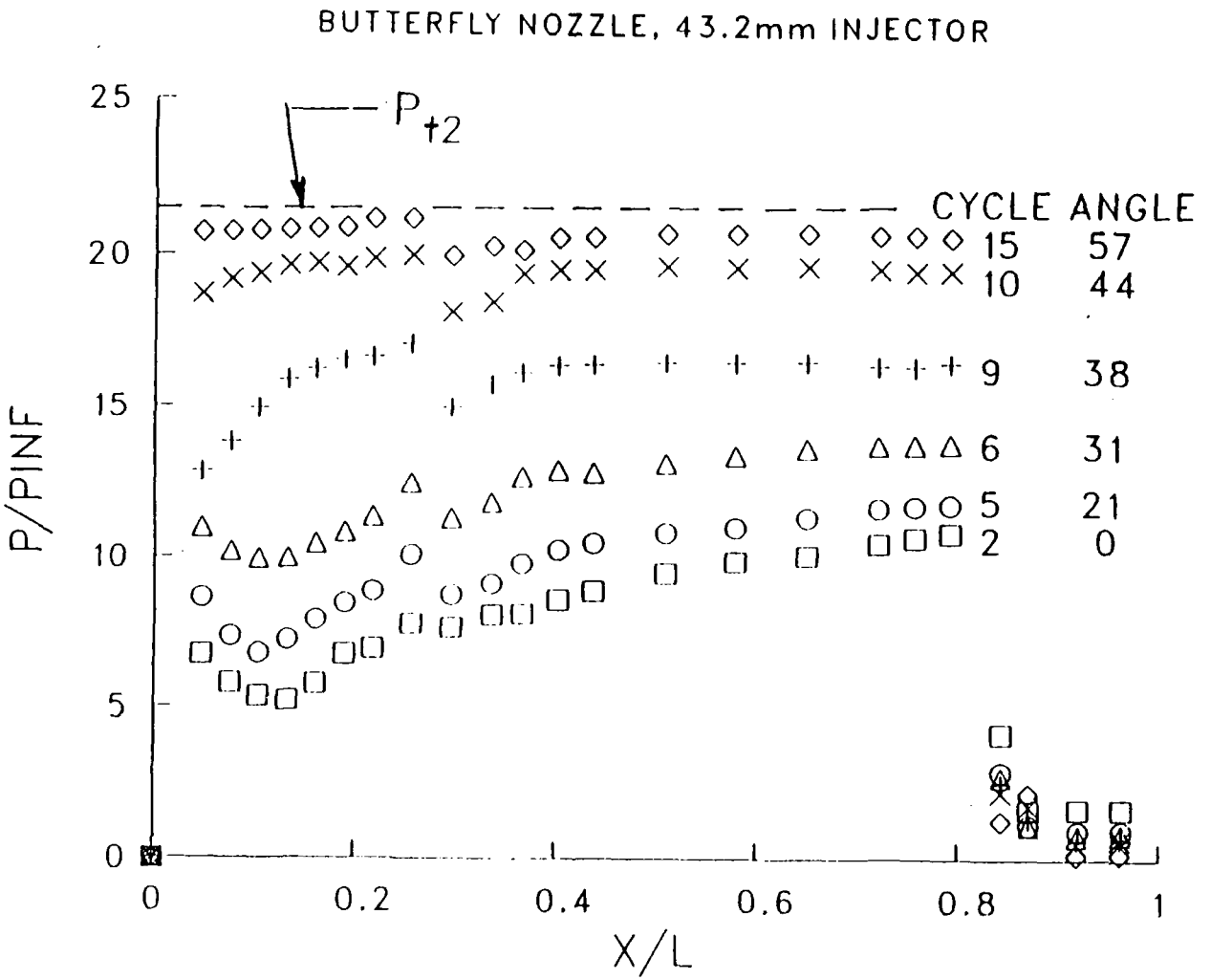

Figure 14. Effect of butterfly valve angle - longitudinal pressure distributions

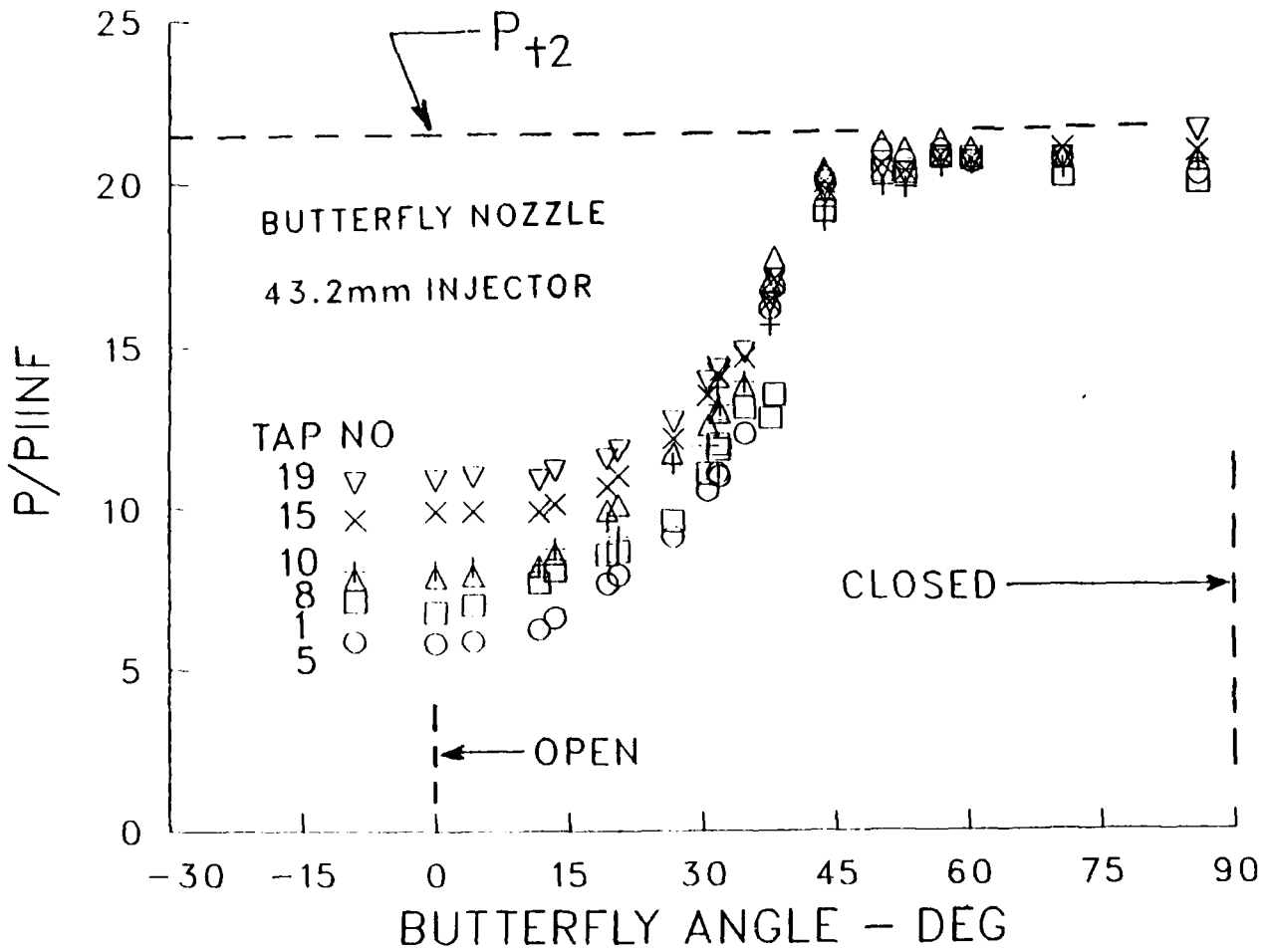

Figure 15. Effect of butterfly valve angle - selected pressure ports

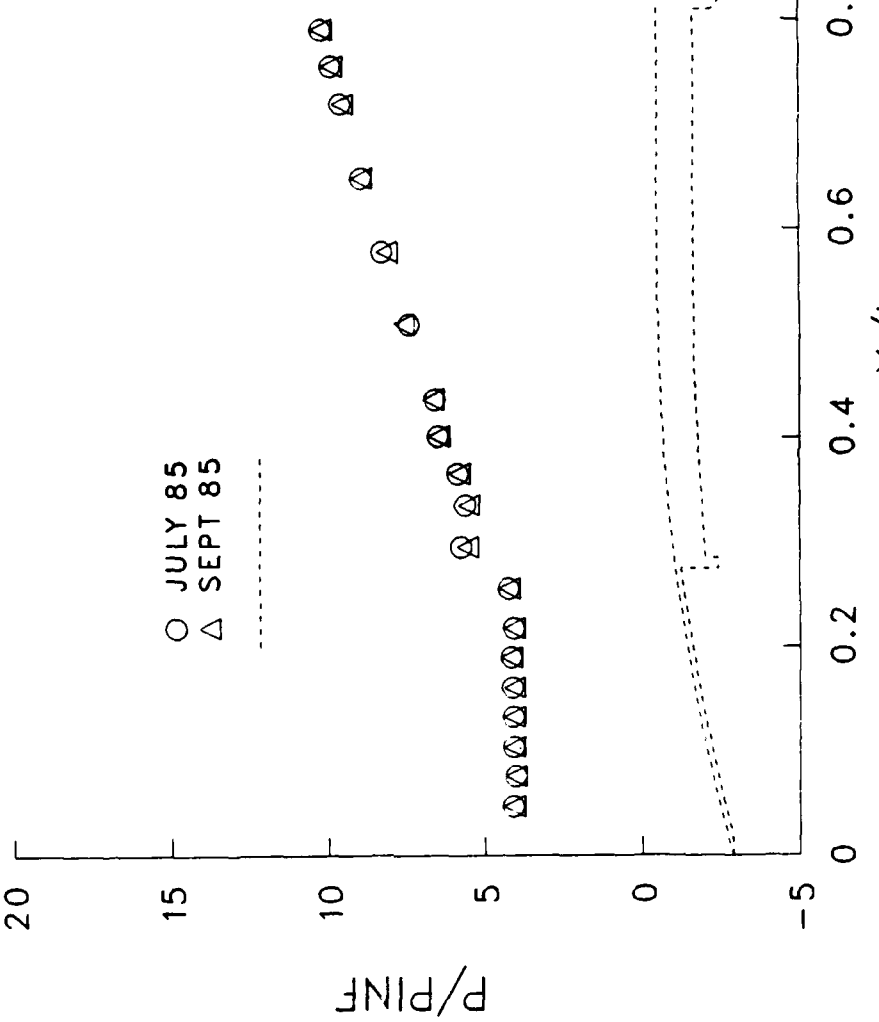

Figure 16. Repeat runs, 39.1 mm nozzle, 43.2mm injector

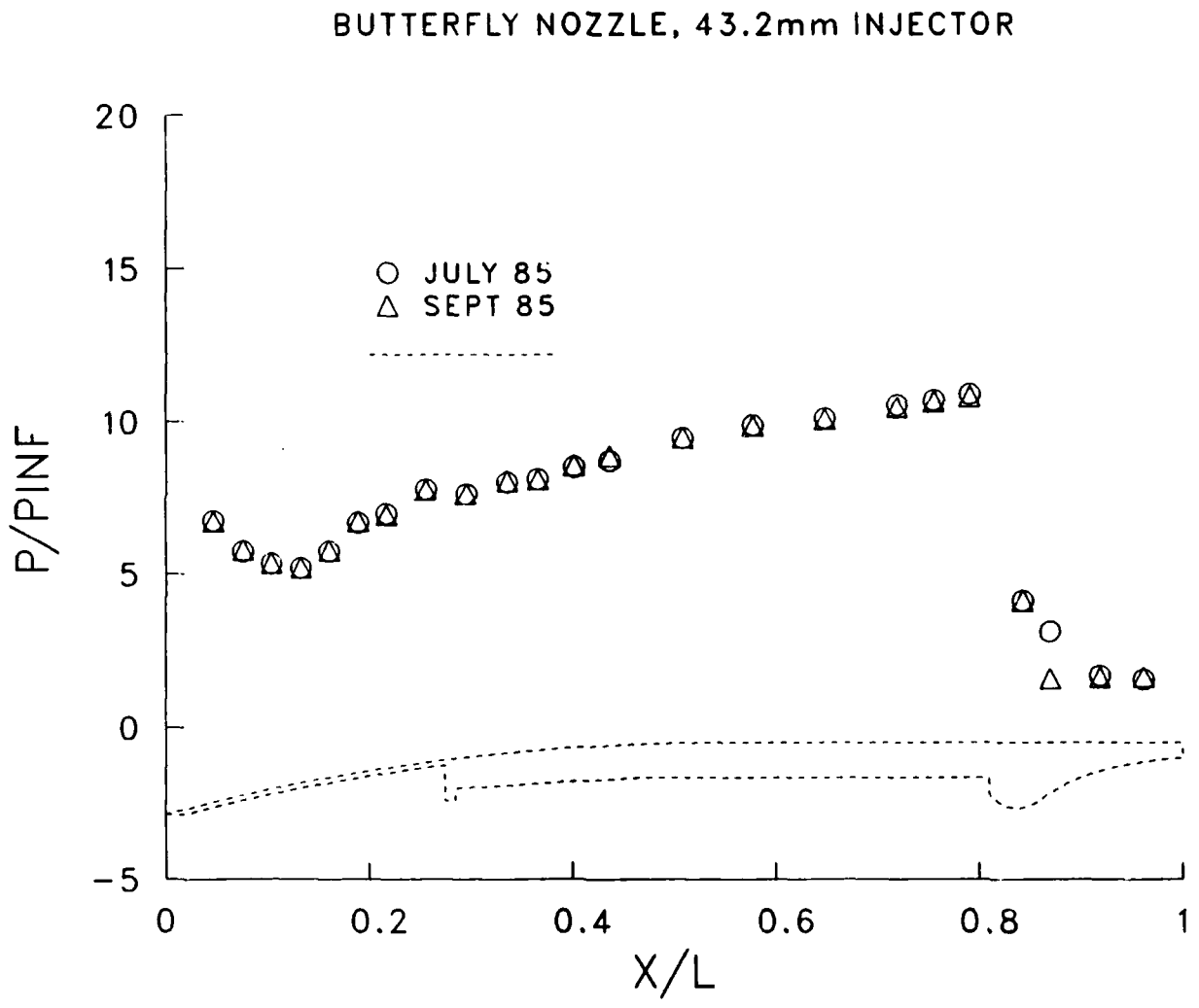

Figure 17. Repeat runs, nozzle with butterfly open, 43.2mm injector

Table 1. Pressure Tap Locations

Inlet		Fuel Section		Nozzle	
	X/L		X/L		X/L
1	.047	9	.296	20	.843
2	.076	10	.336	21	.870
3	.104	11	.366	22	.919
4	.133	12	.402	23	.962
5	.161	13	.437		
6	.190	14	.509		
7	.218	15	.578		
8	.256	16	.649		
9	.296	17	.720		
10	.336	18	.756		
		19	.791		

Table 2. Test Run Summary

No.	RUN-BATCH	INJECTOR	NOZZLE	DATE
1	10-1	43.2mm	BUTTERFLY	JULY 85
2	10-2	43.2mm	BUTTERFLY	"
3	10-3	43.2mm	39.1mm	"
4	10-5	43.2mm	39.1mm	"
5	10-6	43.2mm	NONE	"
6	11-2	43.2mm	39.1mm	SEP 85
7	12-1	43.2mm	40.9mm	"
8	12-3	43.2mm	BUTTERFLY	"
9	12-4	38.1mm	BUTTERFLY	"
10	12-5	38.1mm	39.1mm	"
11	12-6	48.3mm	39.1mm	"
12	13-1	48.3mm	BUTTERFLY	"
13	13-2	VG-6.4mm STP	BUTTERFLY	"
14	13-3	VG-6.4mm STP	39.1mm	"
15	13-4	VG-3.8mm STP/TW	39.1mm	"
16	13-5	VG-3.8mm STP/TW	39.1mm	"
17	13-6	VG-3.8mm STP/TW	BUTTERFLY	"
18	13-7	VG-3.8mm STP	BUTTERFLY	"
19	14-1	VG-3.8mm STP	39.1mm	"
20	14-2	VG-3.8mm STP	40.9mm	"
21	14-3	48.3mm	40.9mm	"
22	14-4	38.1mm	40.9mm	"
23	14-5	VG-6.4mm STP	40.9mm	"
24	14-6	VG-3.8mm STP/TW	40.9mm	"

Table 3. July 1985 Data

RUN BA	10-1	10-2	10-3	10-5	10-5	10-6
INJECT	43.2mm	43.2mm	43.2mm	43.2mm	43.2mm	43.2mm
NOZZ	B'FLY	B'FLY	39.1mm	39.1mm	39.1mm	NONE
CYCLE	4	3	6	2	9	5
p_0 -atm	15.00	14.11	14.18	14.08	14.34	14.22
X/L	p/p_∞	p/p_∞	p/p_∞	p/p_∞	p/p_∞	p/p_∞
0.047	7.079	6.769	4.119	6.686	4.066	0.810
0.076	5.946	5.755	4.035	5.731	3.984	0.666
0.104	5.444	5.351	4.103	5.303	4.096	0.741
0.133	5.322	5.206	4.119	5.173	4.066	0.749
0.161	5.874	5.755	4.134	5.639	4.051	0.749
0.190	6.814	6.708	4.187	6.678	4.126	0.847
0.218	7.086	6.990	4.096	6.915	4.089	0.757
0.256	7.825	7.798	4.247	7.809	4.254	0.817
0.296	7.768	7.638	5.757	7.618	5.724	0.885
0.336	8.112	8.026	5.620	7.970	5.582	0.749
0.366	8.119	8.125	5.863	8.039	5.784	0.454
0.402	8.442	8.529	6.500	8.421	6.482	0.484
0.437	8.736	8.728	6.599	8.726	6.594	0.567
0.509	9.310	9.459	7.425	9.383	7.412	0.658
0.578	9.812	9.886	8.275	9.819	8.283	0.545
0.649	10.084	10.115	8.920	10.010	9.048	0.492
0.720	10.529	10.549	9.610	10.453	9.663	0.409
0.756	10.744	10.709	9.921	10.644	10.001	0.386
0.791	10.945	10.900	10.217	10.820	10.331	0.386
0.843	4.856	4.147	8.093	3.370	3.534	0.129
0.870	3.357	3.140	0.903	0.871	0.923	0.242
0.919	2.231	1.700	1.358	1.352	1.328	0.371
0.962	2.023	1.585	1.744	1.589	1.530	0.288
One atm = 101.3 kPa = 14.69 psia						

Table 4. 39.1mm Nozzle Data, September 1985

RUN BA	12-5	11-2	12-6	13-3	13-4	13-4	14-1	13-5
INJECT	38.1mm	43.2mm	48.3mm	VG/6.4	TWST	TWST	VG/3.8	TWST
NOZZ	39.1mm	39.1mm	39.1mm	39.1mm	39.1mm	39.1mm	39.1mm	39.1mm
CYCLE	7	7	15	11	6	30	20	15
p_0 -atm	14.25	14.36	14.04	14.33	14.48	14.22	14.29	14.41
X/L	p/p_∞	p/p_∞	p/p_∞	p/p_∞	p/p_∞	p/p_∞	p/p_∞	p/p_∞
0.047	8.559	4.075	0.973	8.493	6.796	0.824	8.340	6.703
0.076	6.793	4.030	1.003	6.698	5.920	0.832	6.601	5.882
0.104	6.038	4.068	1.019	5.955	5.467	0.809	5.849	5.426
0.133	5.329	4.075	0.996	5.384	5.445	0.802	5.337	5.382
0.161	5.834	4.068	0.958	5.947	5.913	0.756	5.819	5.874
0.190	6.793	4.180	1.072	7.517	6.796	0.862	7.362	6.733
0.218	8.544	4.068	0.996	8.320	6.975	0.772	8.167	6.942
0.256	9.933	4.225	1.026	9.792	7.680	0.862	9.417	7.621
0.296	6.989	5.543	1.463	6.803	7.420	1.392	7.053	7.397
0.336	7.057	5.498	1.609	7.141	7.725	1.717	7.294	7.636
0.366	7.397	5.798	1.655	7.374	7.740	1.838	7.475	7.710
0.402	7.948	6.457	1.792	7.719	8.186	1.974	7.979	8.166
0.437	8.348	6.629	1.823	7.900	8.483	1.944	8.288	8.427
0.509	9.004	7.581	2.053	8.613	9.292	2.095	9.070	9.240
0.578	9.254	8.105	2.267	8.906	9.649	2.262	9.281	9.666
0.649	9.503	8.892	2.627	9.154	9.961	2.572	9.612	9.912
0.720	9.903	9.536	2.918	9.529	10.399	2.844	10.004	10.382
0.756	10.054	9.873	3.072	9.709	10.637	3.048	10.094	10.599
0.791	10.159	10.195	3.210	9.822	10.756	3.147	10.192	10.711
0.843	3.110	3.521	1.578	3.199	3.320	1.339	3.259	3.336
0.870	0.860	0.936	0.414	0.849	0.899	0.303	0.903	0.873
0.919	1.283	1.348	0.628	1.292	1.344	0.567	1.347	1.314
0.962	1.547	1.700	0.804	1.577	1.627	1.036	1.566	1.605
One atm = 101.3 kPa = 14.69 psia								

Table 5. Butterfly Nozzle Data, Valve Open

RUN BA	12-4	12-3	13-1	13-2	13-6	13-7
INJECT	38.1mm	43.2mm	48.3mm	VG/6.4	TWIST	VG/3.8
NOZZ	B'FLY	B'FLY	B'FLY	B'FLY	B'FLY	B'FLY
CYCLE	3	2	3	3	3	3
p_0 -atm	14.23	14.29	14.17	14.46	14.19	14.29
X/L	p/p_∞	p/p_∞	p/p_∞	p/p_∞	p/p_∞	p/p_∞
0.047	8.600	6.746	4.388	8.530	6.900	8.416
0.076	6.839	5.805	4.343	6.760	6.043	6.684
0.104	6.114	5.368	4.327	6.024	5.550	5.901
0.133	5.434	5.225	4.388	5.518	5.528	5.427
0.161	6.038	5.790	4.350	6.143	5.967	6.022
0.190	7.557	6.754	4.457	7.638	6.839	7.572
0.218	8.615	6.950	4.335	8.434	7.052	8.242
0.256	9.945	7.778	4.403	9.824	7.681	9.492
0.296	7.126	7.642	4.988	6.894	7.514	7.234
0.336	7.194	8.064	5.519	7.199	7.787	7.444
0.366	7.504	8.117	5.975	7.467	7.742	7.648
0.402	8.056	8.584	6.408	7.876	8.257	8.197
0.437	8.426	8.877	6.651	8.077	8.462	8.431
0.509	9.084	9.480	7.341	8.753	9.357	9.191
0.578	9.424	9.864	7.926	8.947	9.690	9.402
0.649	9.703	10.082	8.556	9.252	9.941	9.680
0.720	9.983	10.481	9.194	9.690	10.388	10.094
0.756	10.134	10.669	9.589	9.869	10.638	10.237
0.791	10.172	10.827	9.900	9.891	10.744	10.373
0.843	3.627	4.164	4.403	3.964	3.913	3.846
0.870	1.708	1.611	2.786	2.477	1.964	3.831
0.919	1.383	1.649	1.906	1.577	1.501	1.490
0.962	1.353	1.672	1.989	1.242	1.532	1.521
One atm = 101.3 kPa = 14.69 psia						

Table 6. 40.9mm Nozzle Data, September 1985

RUN BA	14-4	12-1	14-3	14-5	14-6	14-2
INJECT	38.1mm	43.2mm	48.3mm	VG/6.4	TWIST	VG/3.8
NOZZ	1.61	1.61	1.61	1.61	1.61	1.61
CYCLE	20	29	15	25	25	18
p_0 -atm	14.04	14.18	14.29	14.27	14.52	14.26
X/L	p/p_∞	p/p_∞	p/p_∞	p/p_∞	p/p_∞	p/p_∞
0.047	8.132	0.743	0.534	7.815	0.808	7.229
0.076	6.218	0.796	0.557	6.120	0.837	5.901
0.104	5.552	0.774	0.587	5.464	0.808	5.335
0.133	4.977	0.728	0.557	4.899	0.800	4.905
0.161	4.173	0.721	0.557	4.213	0.808	4.482
0.190	5.705	0.865	0.685	5.683	0.897	5.365
0.218	7.642	0.751	0.617	7.589	0.800	7.078
0.256	9.449	0.819	0.655	9.202	0.867	8.760
0.296	5.850	1.350	0.896	5.826	1.037	6.180
0.336	5.927	1.365	1.076	6.384	1.401	6.550
0.366	6.241	1.327	1.408	6.489	1.727	6.625
0.402	6.639	1.441	1.513	6.700	1.815	6.942
0.437	6.884	1.517	1.701	6.843	1.860	7.304
0.509	7.627	1.767	2.017	7.469	2.016	8.104
0.578	8.132	1.927	2.296	8.094	2.193	8.610
0.649	8.339	2.253	2.770	8.268	2.512	8.911
0.720	8.737	2.480	3.094	8.690	2.794	9.206
0.756	8.944	2.655	3.365	8.863	3.001	9.357
0.791	9.105	2.784	3.478	9.059	3.097	9.560
0.843	3.285	1.464	1.776	3.324	1.497	3.463
0.870	1.746	0.379	1.129	2.269	0.600	1.034
0.919	1.432	0.485	1.016	1.409	0.541	1.517
0.962	1.524	0.531	1.272	1.537	0.837	1.668
One atm = 101.3 kPa = 14.69 psia						

Table 7. Longitudinal Pressure Distributions At Different Butterfly Valve Settings

RUN BA	12-3	12-3	12-3	12-3	12-3	12-3
INJECT	43.2mm	43.2mm	43.2mm	43.2mm	43.2mm	43.2mm
NOZZ	B'FLY	B'FLY	B'FLY	B'FLY	B'FLY	B'FLY
ANGLE	0.0	21	31	38	44	57
CYCLE	2	5	6	9	10	15
p_0 -atm	14.29	14.25	14.32	14.15	14.53	14.18
X/L	p/p_∞	p/p_∞	p/p_∞	p/p_∞	p/p_∞	p/p_∞
0.047	6.746	8.650	10.981	12.858	18.716	20.721
0.076	5.805	7.352	10.200	13.846	19.205	20.759
0.104	5.368	6.793	9.975	14.972	19.397	20.797
0.133	5.225	7.238	9.982	15.899	19.649	20.805
0.161	5.790	7.918	10.471	16.257	19.738	20.850
0.190	6.754	8.461	10.846	16.553	19.604	20.873
0.218	6.950	8.869	11.364	16.652	19.878	21.154
0.256	7.778	10.091	12.484	17.093	19.989	21.161
0.296	7.642	8.740	11.304	14.979	18.116	19.948
0.336	8.064	9.110	11.830	15.747	18.442	20.274
0.366	8.117	9.805	12.694	16.150	19.382	20.145
0.402	8.584	10.257	12.912	16.371	19.508	20.547
0.437	8.877	10.484	12.822	16.409	19.501	20.562
0.509	9.480	10.816	13.122	16.470	19.619	20.661
0.578	9.864	10.990	13.392	16.454	19.582	20.661
0.649	10.082	11.337	13.640	16.492	19.627	20.714
0.720	10.481	11.646	13.738	16.363	19.538	20.623
0.756	10.669	11.714	13.760	16.340	19.449	20.630
0.791	10.827	11.775	13.806	16.454	19.471	20.577
0.843	4.164	2.883	2.704	2.509	2.191	1.267
0.870	1.611	1.125	1.119	1.331	1.740	2.177
0.919	1.649	0.921	0.781	0.662	0.540	0.152
0.962	1.672	0.959	0.856	0.730	0.681	0.205
One atm = 101.3 kPa = 14.69 psia						

Table 8. Effect of Butterfly Angle at Selected Port Locations

RUN BA	12-3	12-3	12-3	12-3	12-3	12-3
INJECT	43.2mm	43.2mm	43.2mm	43.2mm	43.2mm	43.2mm
NOZZ	B'FLY	B'FLY	B'FLY	B'FLY	B'FLY	B'FLY
TAP NO	1	5	8	10	14	19
p_0 -atm	14.23	14.23	14.23	14.23	14.23	14.23
BF-ANGLE	p/p_∞	p/p_∞	p/p_∞	p/p_∞	p/p_∞	p/p_∞
-1.200	6.775	5.815	7.879	8.098	9.905	10.873
11.660	7.690	6.246	8.204	8.227	9.905	10.873
20.560	8.665	7.932	10.109	9.126	11.009	11.795
30.600	11.054	10.540	12.567	11.909	13.482	13.897
31.900	11.810	10.971	12.952	13.164	14.049	14.260
34.700	13.103	12.294	13.792	13.897	14.653	14.820
37.600	12.786	16.166	16.997	15.659	16.362	16.362
43.800	19.115	20.158	20.415	18.835	19.999	19.886
53.000	20.287	20.657	21.028	19.856	20.347	20.249
57.050	20.786	20.990	21.322	20.498	20.823	20.740
70.800	20.188	20.725	20.710	20.430	21.012	20.710
85.140	19.969	20.226	20.642	20.627	20.914	21.534
60.500	20.755	20.619	21.028	20.559	20.695	20.612
50.400	20.347	20.952	21.254	19.924	20.536	20.415
43.900	19.145	20.029	20.287	19.251	19.810	19.659
38.100	13.512	16.824	17.738	16.619	17.058	17.020
31.700	11.969	11.070	13.051	13.708	14.147	14.359
26.700	9.610	9.119	11.697	11.402	12.151	12.680
19.300	8.574	7.667	9.950	9.603	10.661	11.531
13.440	8.068	6.608	8.589	8.741	10.124	11.168
4.2400	7.002	5.875	7.909	8.196	9.905	10.971
-9.100	7.123	5.875	7.811	8.068	9.648	10.805

LIST OF SYMBOLS

D_{INJ}	Injector ring hole diameter
$\bar{D}_{INJ}$	Vortex generator equivalent diameter, based on open area
D_{NT}	Nozzle throat diameter
L	Model length
p	Model interior pressures
p_∞	Free-stream static pressure
p_0	Tunnel supply pressure, standard sea level atmospheres
p_{t2}	Total pressure behind a normal shock
X	Axial position measured from inlet leading edge

DISTRIBUTION LIST

No. of Copies	Organization
12	Administrator Defense Technical Info Center ATTN: DTIC-DDA Cameron Station Alexandria, VA 22304-6145
1	HQDA (SARD-TR) Washington, DC 20310
1	Commander US Army Materiel Command ATTN: AMCDRA-ST 5001 Eisenhower Avenue Alexandria, VA 22333-0001
1	Commander US Army Laboratory Command ATTN: AMSLC-TD Adelphi, MD 20783-1145
1	Commander Armament RD&E Center US Army AMCCOM ATTN: SMCAR-MSI Picatinny Arsenal, NJ 07806-5000
1	Commander Armament RD&E Center US Army AMCCOM ATTN: SMCAR-TDC Picatinny Arsenal, NJ 07806-5000
1	Commander Armament RD&E Center US Army AMCCOM ATTN: SMCAR-LC Picatinny Arsenal, NJ 07806-5000
1	Commander Armament RD&E Center US Army AMCCOM ATTN: SMCAR-CAWS-AM (Mr. DellaTerga) Picatinny Arsenal, NJ 07806-5000
3	Commander Armament RD&E Center US Army AMCCOM ATTN: SMCAR-AET-A (R. Kline) SMCAR-FSP-A (F. Scerbo) SMCAR-FSP-A (J. Bera) Picatinny Arsenal, NJ 07806-5000
1	OPM Nuclear ATTN: AMCPM-NUC (COL W. P. Farmer) Dover, NJ 07801-5001
1	Director Benet Weapons Laboratory Armament RD&E Center US Army AMCCOM ATTN: SMCAR-LCB-TL Watervliet, NY 12189
1	Commander US Army Armament, Munitions and Chemical Command ATTN: SMCAR-ESP-L Rock Island, IL 61299
1	Commander US Army Aviation Systems Command ATTN: AMSAV-DACL 4300 Goodfellow Blvd. St. Louis, MO 63120
1	Director US Army Aviation Research and Technology Activity Ames Research Center Moffett Field, CA 94035-1099
1	Commander US Army Communications - Electronics Command ATTN: AMSEL-ED Fort Monmouth, NJ 07703
1	Commander US Army Missile Command ATTN: AMSMI-RD Redstone Arsenal, AL 35898-5000

DISTRIBUTION LIST

No. of Copies	Organization
1	Commander US Army Missile Command ATTN: AMSMI-AS Redstone Arsenal, AL 35898-5000
1	Commander US Army Missile Command ATTN: AMSMI-RDK (Mr. W. Dahlke) Redstone Arsenal, AL 35898-5000
1	Commander US Army Tank Automotive Command ATTN: AMSTA-DI Warren, MI 48090
1	Director US Army TRADOC Analysis Command ATTN: ATAA-SL White Sands Missile Range NM 88002
1	Commandant US Army Infantry School ATTN: ATSH-CD-CSO-OR Fort Benning, GA 31905
1	AFWL/SUL Kirtland AFB, NM 87117
1	Commander US Army Dugway Proving Ground ATTN: STEDP-MT (G. C. Travers) Dugway, UT 84022
1	Commander US Army Yuma Proving Ground ATTN: STEYP-MTW Yuma, AZ 85365-9103
1	Commandant US Army Field Artillery School ATTN: ATSF-GD Fort Sills, OK 73503
1	Director US Army Field Artillery Board ATTN: ATZR-BDW Fort Sills, OK 73503

No. of Copies	Organization
1	Commander Naval Surface Weapons Center ATTN: Dr. W. Yanta Aerodynamics Branch K-24, Bldg. 402-12 White Oak Laboratory Silver Spring, MD 20910
1	Air Force Armament Laboratory ATTN: AFATL/DLODL Eglin AFB, FL 32542-5000
1	Commander Defense Advanced Research Projects Agency ATTN: MAJ R. Lundberg 1400 Wilson Blvd. Arlington, VA 22209
1	Director Lawrence Livermore National Laboratory ATTN: Mail Code L-35 (Mr. T. Morgan) P.O. Box 808 Livermore, CA 94550
2	Director Sandia National Laboratories ATTN: Dr. W. Oberkampf Dr. W. P. Wolfe Division 1636 Albuquerque, NM 87185
1	Director National Aeronautics and Space Administration Langley Research Center ATTN: Technical Library Langley Station Hampton, VA 23365
1	Director National Aeronautics and Space Administration Langley Research Center ATTN: Dr. G.B. Northam Hampton, VA 23665

DISTRIBUTION LIST

No. of Copies	Organization
1	Director National Aeronautics and Space Administration Ames Research Center ATTN: Dr. J. Steger Moffett Field, CA 94035
1	Aerospace Corporation Aero-Engineering Subdivision ATTN: Walter F. Reddall El Segundo, CA 90245
1	Calspan Corporation ATTN: W. Rae P.O. Box 400 Buffalo, NY 14225
1	Interferometrics, Inc. ATTN: Mr. R. F. L'Arriva 8150 Leesburg Pike Vienna, VA 22180
3	Rockwell International Science Center ATTN: Dr. V. Shankar Dr. S. Chakravarthy Dr. U. Goldberg 1049 Camino Dos Rios P.O. Box 1085 Thousand Oaks, CA 91360
2	United Technologies Corporation Chemical Systems Division ATTN: Dr. R. O. MacLaren Mr. A. L. Holzman 600 Metcalf Road, P.O. Box 50015 San Jose, CA 95150-0015
1	Arizona State University Department of Mechanical and Energy Systems Engineering ATTN: Dr. G.P. Neitzel Tempe, AZ 85281
1	University of California - Davis ATTN: Dr. Harry A. Dwyer Davis, CA 95616

Aberdeen Proving Ground

Director, USAMSAA
ATTN: AMXSY-D
AMXSY-MP, H. Cohen
AMXSY-RA, R. Scungio

Commander, USATECOM
ATTN: AMSTE-TO-F
AMSTE-TE-F, W. Vomocil

PM-SMOKE, Bldg. 324
ATTN: AMCPM-SMK-M
J. Callahan

Commander, CRDEC, AMCCOM
ATTN: SMCCR-RSP-A
M.C. Miller
D. Olson
SMCCR-MU
W. Dee
C. Hughes
D. Bromley
SMCCR-SPS-IL

USER EVALUATION SHEET/CHANGE OF ADDRESS

This laboratory undertakes a continuing effort to improve the quality of the reports it publishes. Your comments/answers below will aid us in our efforts.

1. Does this report satisfy a need? (Comment on purpose, related project, or other area of interest for which the report will be used.) _____

2. How, specifically, is the report being used? (Information source, design data, procedure, source of ideas, etc.) _____

3. Has the information in this report led to any quantitative savings as far as man-hours or dollars saved, operating costs avoided, or efficiencies achieved, etc? If so, please elaborate. _____

4. General Comments. What do you think should be changed to improve future reports? (Indicate changes to organization, technical content, format, etc.) _____

BRL Report Number _____ Division Symbol _____

Check here if desire to be removed from distribution list. ____

Check here for address change. ____

Current address: Organization _____
Address _____

----------FOLD AND TAPE CLOSED----------

Director
U.S. Army Ballistic Research Laboratory
ATTN: SLCBR-DD-T(NEI)
Aberdeen Proving Ground, MD 21005-5066

OFFICIAL BUSINESS
PENALTY FOR PRIVATE USE $300

BUSINESS REPLY LABEL
FIRST CLASS PERMIT NO. 12062 WASHINGTON D.C

POSTAGE WILL BE PAID BY DEPARTMENT OF THE ARMY

NO POSTAGE NECESSARY IF MAILED IN THE UNITED STATES

Director
U.S. Army Ballistic Research Laboratory
ATTN: SLCBR-DD-T(NEI)
Aberdeen Proving Ground, MD 21005-9989